ELSEVIER

Ceramics International 29 (2003) 299–304

CERAMICS INTERNATIONAL

www.elsevier.com/locate/ceramint

Mechanical and electrical properties of B_4C–CrB_2 ceramics fabricated by liquid phase sintering

Suzuya Yamada[a,*], Kiyoshi Hirao[b], Yukihiko Yamauchi[b], Shuzo Kanzaki[b]

[a]*Synergy Ceramics Laboratory, Fine Ceramics Research Association, Nagoya, Aichi 463-8687, Japan*
[b]*Synergy Materials Research Center, National Institute of Advanced Industrial Science and Technology, Nagoya, Aichi 463-8687, Japan*

Received 15 April 2002; received in revised form 7 May 2002; accepted 8 June 2002

Abstract

B_4C based ceramic composites with additions of CrB_2 up to 25 mol% were fabricated by hot pressing at 2050 °C with a low applied load of 5 MPa. The CrB_2 addition enhanced the densification of B_4C due to the formation of CrB_2 –B_4C eutectic liquid. Both a high strength of 684 MPa and a modest fracture toughness of 3.2 MPa $m^{1/2}$ were obtained for the B_4C– 22.5 mol% CrB_2 specimen. Furthermore, the electrical conductivity was increased remarkably for the specimens with more than 15 mol% CrB_2, which was attributed to the formation of three-dimensional network of the electrically conductive CrB_2 phase.

Keywords: C. Mechanical properties; C. Electrical conductivity; D. Carbide; Composite ceramic

1. Introduction

Boron carbide (B_4C) has excellent properties for an engineering material, such as extreme hardness, a high elastic modulus, a high melting point, good chemical stability, and a high neutron absorption cross section. Furthermore, B_4C ceramics have high erosion and abrasion resistance [1–5]. They are employed in nuclear energy and high-temperature thermoelectric conversion as well as erosive-wear applications such as nozzles. However, their range of applications is restricted by their low strength and fracture toughness as well as poor sinterability and machinability. Fully densified B_4C ceramics without additives are usually fabricated by means of hot pressing above 2100 °C with an applied load of more than 30 MPa [13], which is relatively expensive. The addition of carbon was found to be an effective sintering additive for B_4C [6–10]. A B_4C ceramic with a relative density of 96.4% was pressureless-sintered at 2150 °C with the addition of carbon [10]. By means of a post-HIP treatment for this material, full densification could be achieved. A flexural strength of 579 MPa and a fracture toughness of 2.4 MPa $m^{1/2}$ were obtained for the post-HIPed specimen. Aluminium and Al-containing compounds such as AlF_3 and Al_2O_3 were also found to be effective for the densification of B_4C [11,12]. The sinterability was remarkably improved by the addition of a small amount of Al_2O_3, and a flexural strength of 550 MPa was obtained for a B_4C ceramic fabricated by hot-pressing of a B_4C powder with 2.5 vol.% Al_2O_3 at 2000 °C [12]. The effects of other additives such as SiC, TiC, WC and BN were also examined, with limited success [13–16].

The purpose of the investigations mentioned above was mainly to promote the densification and to increase the strength of B_4C ceramics. On the contrary, B_4C–TiB_2 composites were investigated to improve both strength and toughness [17,18]. The improvement of fracture toughness by the addition of TiB_2 was explained in terms of microcrack formation caused by the thermal expansion mismatch of dispersed particles of TiB_2 and the B_4C matrix [17–19]. Skorokhod and Krstic fabricated a B_4C–TiB_2 composite with a flexural strength of 621 MPa and a fracture toughness of 6.1 MPa $m^{1/2}$ by reaction-hot pressing of B_4C powder with the addition of TiO_2 and C at 2000 °C [18]. We have reported that a B_4C–20 mol% CrB_2 composite with both a high strength of 630 MPa and a modest fracture

* Corresponding author at: Research Center, Denki Kagaku Kogyo K.K., 3-5-1 Asahi-cho, Machida-city, Tokyo 194-8560, Japan. Tel.: +81-42-721-3642; fax: +81-42-721-3693.
E-mail address: suzuya-yamada@denka.co.jp (S. Yamada).

0272-8842/03/$22.00
PII: S0272-8842(02)00120-7

toughness of 3.5 MPa $m^{1/2}$ could be obtained by hot-pressing powder mixtures of fine B_4C and CrB_2 at 1900 °C with an applied load of 50 MPa [22, 23].

Liquid phase sintering is expected to be an alternative method for fabricating dense B_4C ceramics with improved mechanical properties, analogous to the densification of non-oxide ceramics with high covalency, such as silicon carbide and silicon nitride [24,25]. It was reported that the addition of a small amount of Fe enhanced the densification of B_4C–TiB_2 composites due to the formation of an iron-rich liquid phase [17, 20]. Tuffe et al. fabricated a B_4C–50 mass% TiB_2 composite with a flexural strength of 620 MPa and a fracture toughness of 5.7 MPa $m^{1/2}$ by hot pressing with the addition of 0.5 mass% Fe at 1800 °C [17]. However, research on the liquid phase sintering of B_4C based ceramics is very limited.

In our previous work [24,25], the B_4C–CrB_2 composites were fabricated without a liquid phase during hot pressing, since the sintering temperature of 1900 °C was lower than the eutectic temperature of the CrB_2–B_4C system [26]. At higher sintering temperature, liquid phase sintering is expected to occur by the formation of a CrB_2–B_4C eutectic liquid phase. In addition, as CrB_2 has high electrical conductivity, it was expected that conductivity of the composite material could be increased to such a degree that electrical discharge machining would be available. In the present study, the B_4C–CrB_2 composites were fabricated by liquid phase sintering with a low applied load, and the mechanical and electrical properties of the specimens were examined and compared with the monolithic B_4C.

2. Experimental procedure

Fig. 1 shows SEM photographs of starting powders. The B_4C starting powder (Grade 3000F, Elektroschmelzwerk Kempten GmbH, Munich, Germany) has a mean particle size of 0.43 μm and a specific surface area of 15.3 m^2/g. The powder contained oxygen (2.0 mass%), Fe (140 ppm) and Al (50 ppm) as impurities. The B_4C powder was mixed with CrB_2 powder with a mean particle size of 3.5 μm (Japan New Metals Co., Osaka, Japan) using a planetary ball mill with a SiC pot and SiC balls in methanol for 30 min. The amount of CrB_2 varied from 5 to 25 mol%. The slurry was dried in a rotary vacuum evaporator for 1 h, followed by oven-drying at 115 °C for 24 h. The powder mixture was passed through a 60-mesh sieve. Hot pressing was performed using a carbon resistance furnace in a rectangular graphite die (47×42 mm) at 2050 °C for 1 h with a low applied load of 5 MPa in a flowing Ar atmosphere. The temperature was monitored by an optical pyrometer, which was calibrated in advance using a thermocouple. The heating rates were 40 °C/min from room temperature to 1200 °C, 20 °C/min to 1500 °C and 10 °C/min to 2050 °C. For the sake of comparison, the B_4C specimen without CrB_2 was also fabricated by the same procedure.

For measuring the mechanical properties, test pieces were cut from the hot-pressed specimens and ground with a 400-grit diamond wheel to dimensions of 42×4×3 mm. The flexural strength was measured by a four-point bending test with inner and outer spans of 10 and 30 mm, respectively. The fracture toughness, K_{IC}, was measured by the SEPB method [21]. The densities of test pieces were determined by the Archimedes' method. Phase identification was performed by X-ray diffractometry (XRD: RINT 2500, Rigaku Co, Tokyo, Japan) with Cu$K\alpha$ radiation. In order to observe the microstructure, specimens were polished with a 1 μm diamond slurry. Some specimens were etched with Murakami's reagent (10 g of NaOH and 10 g of $K_3Fe(CN)_6$ in 100 ml H_2O at 110 °C). Microstructural analysis was carried out using scanning electron microscopy (SEM: JSM5600, Jeol Ltd., Tokyo, Japan). The mean grain size of B_4C was measured using image analysis (Scion Image, Scion Co., Maryland, USA). The ultrasonic pulse method was employed to measure the

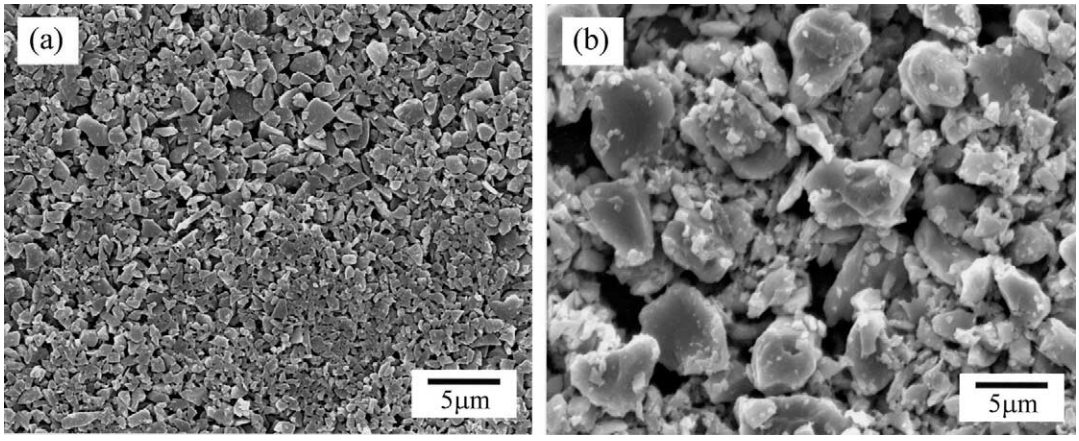

Fig. 1. SEM photographs of starting powders: (a) B_4C powder and (b) CrB_2 powder.

elastic modulus. The electrical conductivity was measured by the four-probe method.

3. Results and discussion

Table 1 summarises starting compositions and their theoretical densities calculated based on the densities of each compound. Fig. 2 shows the relative densities of specimens hot-pressed at 2050 °C as a function of the CrB_2 content. The relative density of the monolithic B_4C specimen was as low as 79.3%. The sinterability was improved by the addition of CrB_2. The relative densities of the B_4C–CrB_2 specimens increased with increasing the CrB_2 content. With the addition of more than 10 mol% CrB_2, high relative densities of over 95% were obtained. In particular, the highest value of 98.0% could be achieved for the specimen with 22.5 mol% CrB_2.

Fig. 3 shows the X-ray diffraction patterns of the B_4C–5 mol% CrB_2 and B_4C–20 mol% CrB_2 specimens. Only the B_4C and CrB_2 phases were identified, except for a small peak at 35.7 °C, which corresponds to diffraction from SiC (102). This SiC contamination is thought to originate from the SiC pot and balls during mixing. Therefore, the B_4C–CrB_2 composite specimens were composed of B_4C and CrB_2 phases with a trace of SiC.

Fig. 4 shows the microstructures of the B_4C composite specimens with 5, 10, 20 and 22.5 mol% CrB_2 observed in the polished surfaces of the specimens. The CrB_2 phase appears as areas of high contrast in the darker B_4C phase. It can be seen that the size and the number of pores decreased with increasing the CrB_2 content. The morphology and size of the CrB_2 phase of the B_4C–CrB_2 specimens were quite different from those of the CrB_2 starting powder (Fig. 1b) and it seems that the CrB_2 penetrated among the fine equiaxed B_4C grains. Therefore, it is apparent that a liquid phase formed in the B_4C–CrB_2 system during sintering at 2050 °C, although the eutectic temperature for the B_4C–CrB_2 system was 2150 °C [26]. It is considered that

Table 1
Starting compositions and theoretical densities

No.	Starting composition				Theoretical density (g/cm^3)
	B_4C	CrB_2	B_4C	CrB_2	
	mol%		vol.%		
1	100	0	100	0	2.52
2	90	10	93.8	6.2	2.71
3	85	15	90.4	9.6	2.82
4	80	20	87.0	13.0	2.92
5	77.5	22.5	85.2	14.8	2.98
6	75	25	83.3	16.7	3.03

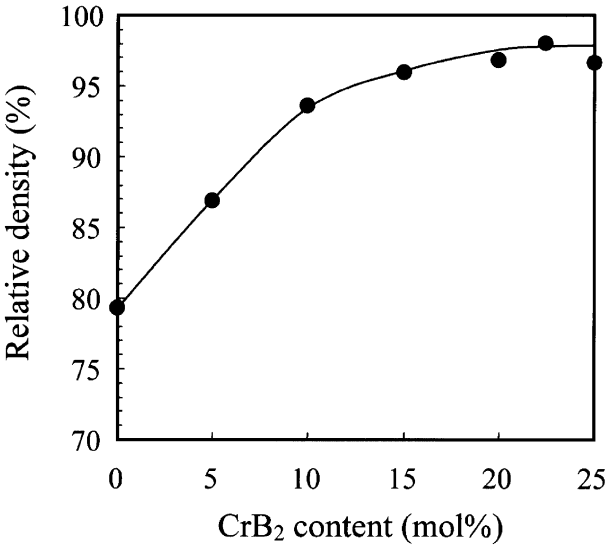

Fig. 2. Relative densities of specimens as a function of CrB_2 content.

impurities in the raw powders or the deviation from the stoichiometry of B_4C lowers the eutectic temperature of the system. In order to clarify the grain morphology of the B_4C phase in the composites, chemical etching was conducted. Fig. 5 shows a polished and chemically etched surface of the B_4C–20 mol% CrB_2 specimen. Large pores were formed by dissolution of CrB_2 during etching. This composite specimen was composed of fine equiaxed grains with a mean size of 1.75 μm in diameter. The grain size of the B_4C in the composite specimen was not significantly changed compared to that of the starting powder (Fig. 1a). The densification was, therefore, mainly attributed to B_4C particle rearrangement by the CrB_2–B_4C eutectic liquid phase. It seems that the liquid phase enhanced the densification, therefore, the relative densities of specimens increased with increasing the CrB_2 content.

The flexural strength and fracture toughness of the specimens as a function of the CrB_2 content are shown in Fig. 6. The flexural strength and the fracture

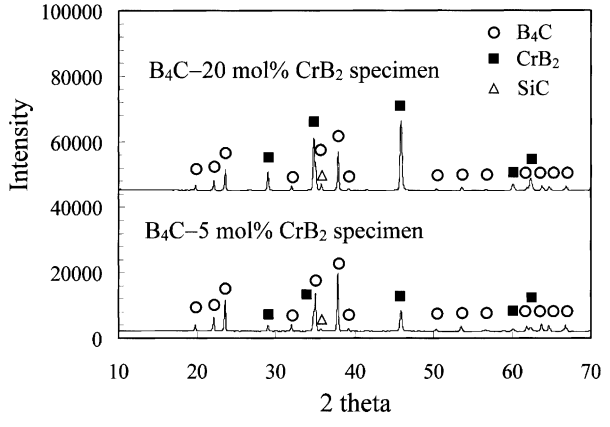

Fig. 3. X-ray diffraction patterns of B_4C–CrB_2 specimens.

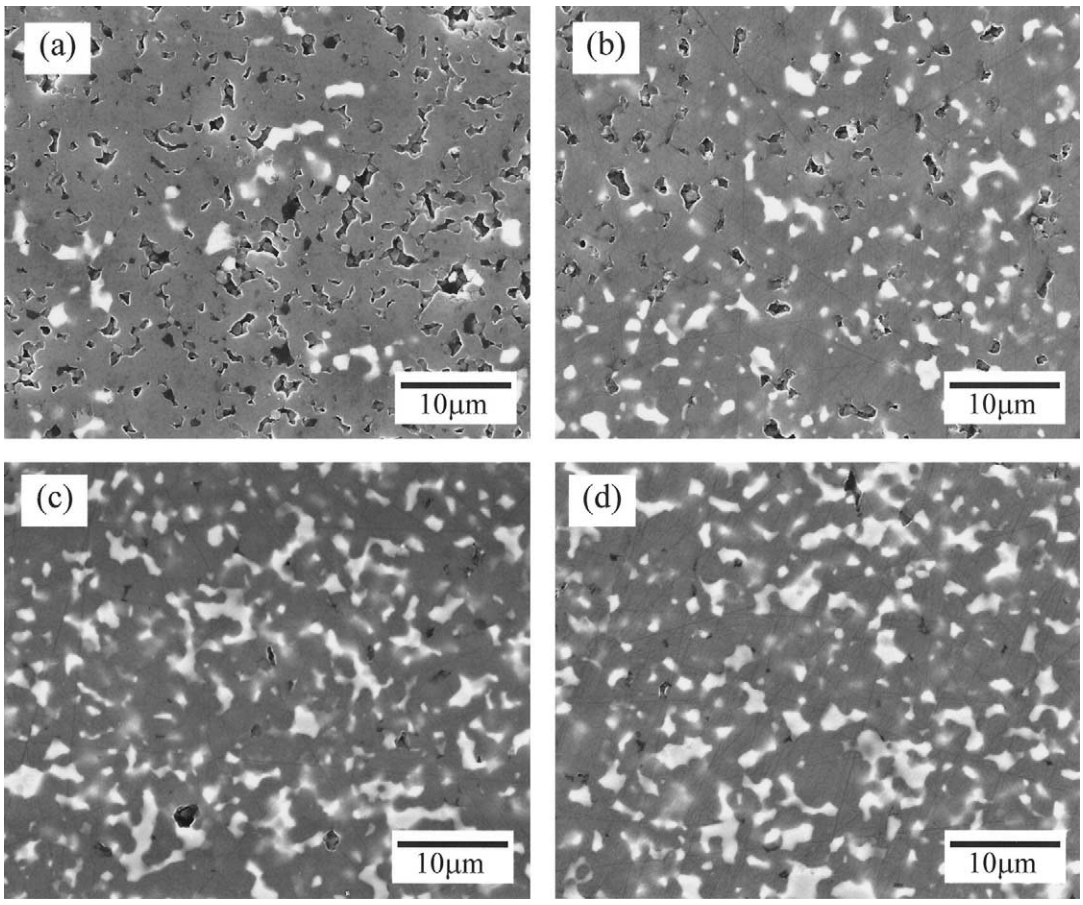

Fig. 4. Microstructures of B_4C–CrB_2 specimens: (a) B_4C–5 mol% CrB_2, (b) B_4C–10 mol% CrB_2, (c) B_4C–20 mol% CrB_2 and (d) B_4C–22.5 mol%

toughness of the specimens with CrB_2 content less than 10 mol% were very low due to insufficient densification. The fracture toughness increased to 3.2 MPa $m^{1/2}$ with increasing the CrB_2 content up to 20 mol% (13.0 vol%), and thereafter it tended to be saturated (Fig. 6b). The reported fracture toughness of monolithic B_4C with nearly full density was 2.5–2.8 MPa $m^{1/2}$ [10,22,23].

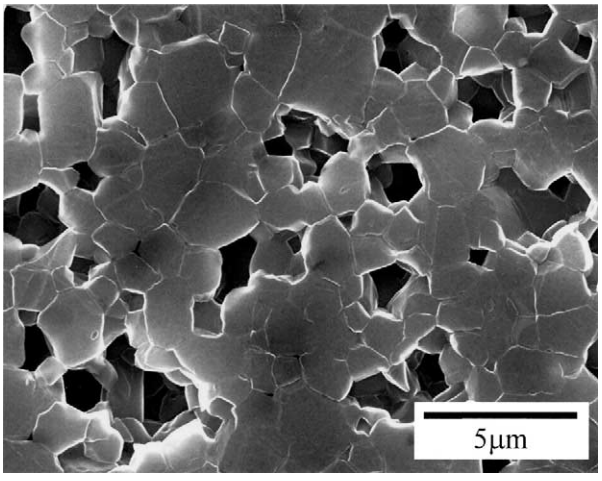

Fig. 5. Microstructure of B_4C–20 mol% CrB_2 specimen.

When these values were compared with those of the composite specimens with R. D. > 95%, it can be said that the fracture toughness of the monolithic B_4C was improved by the addition of CrB_2. The improvement in fracture toughness for the B_4C–CrB_2 specimens can be explained in terms of the residual stress around the CrB_2 phase. The thermal expansion coefficient of CrB_2 is larger than that of B_4C [1], and, as a result, residual stress is generated around the CrB_2 phase during cooling. It seems that this residual stress results in the formation of microcracks and, to some degree, the deflection of propagating cracks, leading to improved fracture toughness of the composite materials [17–19,27]. The addition of CrB_2 also increased the flexural strength, as shown in Fig. 6a. A high strength of over 600 MPa was obtained for CrB_2 contents of 20–25 mol%. In particular, the highest flexural strength of 684 MPa and a modest fracture toughness of 3.2 MPa $m^{1/2}$ could be achieved for the specimen with 22.5 mol% CrB_2. The improvement in strength by the addition of CrB_2 was apparently due to the densification, which led to a reduction in the number and size of the pores acting as the fracture origins.

The elastic modulus of specimens as a function of CrB_2 content is shown in Fig. 7. Since the pores in a

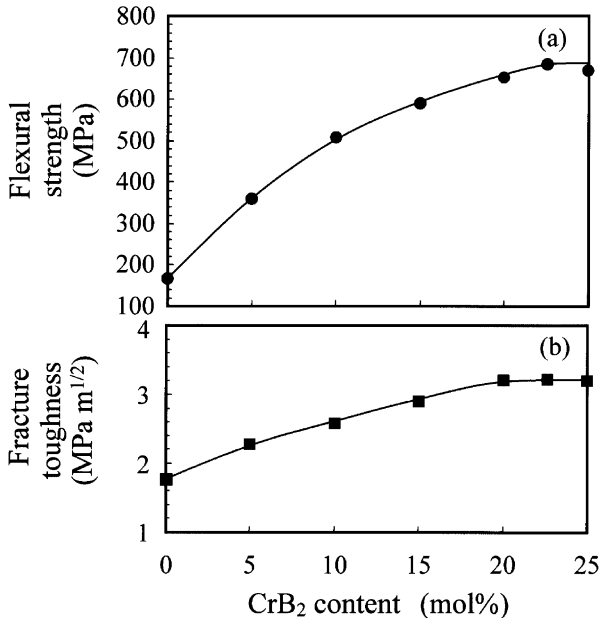

Fig. 6. Mechanical properties of specimens as a function of CrB_2 content:(a) flexural strength and (b) fracture toughness.

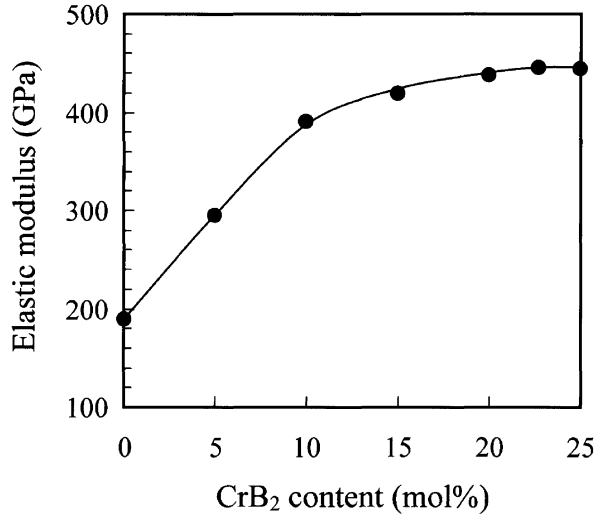

Fig. 7. Elastic modulus of specimens as a function of CrB_2 content.

sintered material have a detrimental effect on the elastic modulus, the improvement in densification by the addition of CrB_2 remarkably increased the elastic modulus. An elastic modulus of about 445 GPa was achieved for the specimens with 22.5–25 mol% CrB_2. These values were almost the same as those of 454 GPa for the monolithic B_4C [22].

Fig. 8 shows the electric conductivity of specimens as a function of the CrB_2 content. The estimated electric conductivity based on Maxwell's equation is also shown in this figure by dotted line. In this calculation, it was assumed that the electric conductivities for B_4C and CrB_2 were 120 S/m [22] and 1.2×10^6 S/m [1], respectively. The electric conductivity of the specimen without

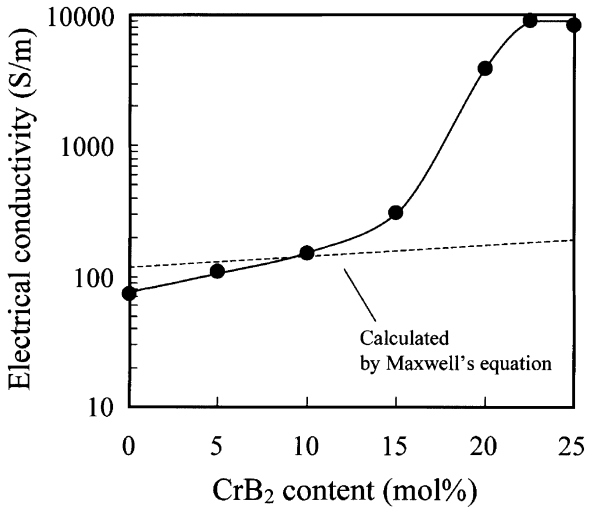

Fig. 8. Electrical conductivity of specimens as a function of CrB_2 content.

CrB_2 was as low as 74 S/m due to insufficient densification. The electric conductivity of the B_4C–CrB_2 specimens increased slightly to 300 S/m with increasing the CrB_2 content up to 15 mol%. However, a marked improvement occurred with CrB_2 content between 15 mol% (9.6 vol.%) and 20 mol% (13.0 vol.%). A high electric conductivity of about 9×10^3 S/m was obtained for the specimens with 22.5–25 mol% CrB_2, which is much higher than the value estimated assuming the isolated dispersion of the second phase. Therefore, the rapid increase in the electric conductivity was ascribed to the formation of the three-dimensional network of the CrB_2 phase with a high electric conductivity. As a result of this improvement in electric conductivity, electric discharge machining can be achieved.

4. Conclusions

B_4C–CrB_2 ceramic composites were fabricated by hot pressing of a powder mixture of B_4C and CrB_2 at 2050 °C with a low applied load of 5 MPa. The densification of B_4C was enhanced by the addition of CrB_2 due to the liquid phase formation, and therefore, the elastic modulus was increased. The fracture toughness was improved, a change that was ascribed to the densification and residual stress caused by the thermal expansion mismatch of CrB_2 and B_4C. As a result of this improvement in densification and fracture toughness, the flexural strength was greatly increased. A B_4C–CrB_2 composite with a both high strength of 684 MPa and a modest fracture toughness of 3.2 MPa m$^{1/2}$ could be obtained by the addition of 22.5 mol% CrB_2. Moreover, the CrB_2 addition also remarkably increased the electrical conductivity at a content of more than 15 mol% CrB_2, since a three-dimensional network of the CrB_2 phase was formed.

Acknowledgements

This work has been supported by METI, Japan, as part of the Synergy Ceramics Project. Part of the work has been supported by NEDO. The authors are members of the Joint Research Consortium of Synergy Ceramics. The authors are grateful to Dr. Shuji Sakaguchi (AIST) for his valuable comments.

References

[1] H. Nishikawa, Powder or boron compound at present, Ceramics 22 (1) (1987) 40–45.
[2] K. Takagi, Boride materials, Metals and Technologies 1 (1993) 23–28.
[3] K. Nishiyama, Sintering and tribology of boride hard materials, J. Jpn. Soc. Powder Powder Metall. 43 (4) (1996) 464–471.
[4] W.C. Johnson, Am. Ceram. Soc. Bull. 80 (6) (2001) 64–66.
[5] P. Larsson, N. Axen, S. Hogmark, Improvements of the microstructure and erosion resistance of boron carbide with additives, J. Mater. Sci. 35 (2000) 3433–3440.
[6] F. Thevenot, Boron carbide—a comprehensive review, J. Eur. Ceram. Soc. 6 (1990) 205–225.
[7] F. Thevenot, A review on boron carbide, Key Eng. Mater. 56–57 (1991) 59–88.
[8] H. Suzuki, T. Hase, T. Maruyama, Effect of carbon on sintering of boron carbide, Yogyo-Kyokai-Shi 87 (8) (1979) 430–433.
[9] K.A. Schwetz, W. Grellner, The influence of carbon on the microstructure and mechanical properties of sintered boron carbide, J. Less-Common Met. 82 (1981) 37–47.
[10] K.A. Schwetz, L.S. Sigl, L. Pfau, Mechanical properties of injection molded B_4C–C ceramics, J. Solid State Chem. 133 (1997) 68–76.
[11] Y. Kanno, K. Kawase, K. Nakano, Additive effect on sintering of boron carbide, Yogyo-Kyokai-Shi 95 (11) (1987) 1137–1140.
[12] H.W. Kim, Y.H. Koh, H.E. Kim, Densification and mechanical properties of B_4C with Al_2O_3 as a sintering aid, J. Am. Ceram. Soc. 83 (11) (2000) 2863–2865.
[13] F. Thevenot, Sintering of boron carbide and boron carbide silicon carbide two phase materials and their properties, J. Nucl. Mater. 152 (1988) 154–162.
[14] L.S. Sigl, Processing and mechanical properties of boron carbide sintered with TiC, J. Eur. Ceram. Soc. 18 (1998) 1521–1529.
[15] Z. Zakhariev, D. Radev, Properties of polycrystalline boron carbide sintered in the presence of W_2B_5 without pressing, J. Mater. Sci. Lett. 7 (1988) 695–696.
[16] R. Ruh, M. Kearns, A. Zangvil, Y. Xu, Phase and property studies of boron carbide–boron nitride composites, J. Am. Ceram. Soc. 75 (4) (1992) 864–872.
[17] S. Tuffe, J. Dubois, G. Fantozzi, G. Barbier, Densification, microstructure and mechanical properties of TiB_2–B_4C based composites, Int. J. Refr. Metals Hard Mater. 14 (1996) 305–310.
[18] V. Skorokhod, V.D. Krstic, High strength-high toughness B_4C–TiB_2 composites, J. Mater. Sci. Lett. 19 (2000) 237–239.
[19] L.S. Sigl, H.J. Kleebe, Microcracking in B_4C–TiB_2 composites, J. Am. Ceram. Soc. 78 (9) (1995) 2374–2380.
[20] D.K. Kim, C.H. Kim, Pressureless sintering and microstructural development of B_4C–TiB_2 based composites, Adv. Ceram. Mater. 3 (1) (1988) 52–55.
[21] T. Nose, T. Fujii, Evaluation of fracture toughness for ceramic materials by a single-edge-precracked-beam method, J. Am. Ceram. Soc. 71 (5) (1988) 328–333.
[22] S. Yamada, Y. Yoshizawa, M. Toriyama, Mechanical properties of boron carbide ceramics, in: Proceedings of the 7th International Conference on Ceramics Processing Science, 2000, pp. 683–688.
[23] S. Yamada, K. Hirao, Y. Yamauchi, S. Kanzaki, Mechanical properties of boron carbide ceramics, in: Proceedings of the 25th Annual Conference on Composites, Advanced Ceramics, Materials, and Structures: A, 2001, pp. 215–220.
[24] M. Omori, H. Takei, Pressureless sintering of SiC, J. Am. Ceram. Soc. 65 (6) (1982) C–92.
[25] E. Tani, S. Umebayashi, K. Kishi, K. Kobayashi, M. Nishijima, Gas-pressure sintering of Si_3N_4 with concurrent addition of Al_2O_3 and 5 wt.% rare earth oxide: high fracture toughness Si_3N_4 with fiber-like structure, Am. Ceram. Soc. Bull. 65 (9) (1986) 1311–1315.
[26] S.S. Ordanyan, A.I. Dmitriev, Reaction in the B_4C–B_2Cr system, in: Villars, A. Prince, H. Okamoto (Eds.), Handbook of Ternary Alloy Phase Diagrams, Vol. 5, ASM International, OH, 1995, pp. 5327.
[27] M. Yasuoka, M.E. Brito, K. Hirao, S. Kanzaki, Effect of dispersed particle size on mechanical properties of alumina/non-oxides composites, J. Ceram. Soc. Jpn. 101 (8) (1993) 889–894.